

Article

Removal of Persistent Acid Pharmaceuticals by a Biological-Photocatalytic Sequential Process: Clofibric Acid, Diclofenac, and Indomethacin

María J. Cruz-Carrillo ¹, Rosa M. Melgoza-Alemán ^{1,*}, Cecilia Cuevas-Arteaga ² and José B. Proal-Nájera ^{3,*} 

¹ Facultad de Ciencias Químicas e Ingeniería, Universidad Autónoma del Estado de Morelos, Av. Universidad 1001, Col. Chamilpa, Cuernavaca 62209, Mexico

² Centro de Investigación en Ingenierías y Ciencias Aplicadas, Universidad Autónoma del Estado de Morelos, Av. Universidad 1001, Col. Chamilpa, Cuernavaca 62209, Mexico

³ Instituto Politécnico Nacional, CIIDIR-Unidad Durango, Calle Sigma 119, Fracc. 20 de Noviembre II, Durango 34220, Mexico

* Correspondence: rmelgoza@uaem.mx (R.M.M.-A.); jproal@ipn.mx (J.B.P.-N.)

Abstract: The removal of three acid pharmaceuticals—clofibric acid (CLA), diclofenac (DCL), and indomethacin (IND)—by a biological-photocatalytic sequential system was studied. These pharmaceutical active compounds (PhACs) are considered to persist in the environment and have been found in water and sewage, producing adverse effects on the aquatic environment. For the biological process, in batch experiments, a fixed bed bioreactor and activated sludge (hybrid bioreactor), under aerobic conditions, was used as pretreatment. The pretreated effluent was exposed to a photocatalytic process employing TiO₂ nanotubular films (NTF-TiO₂) with the following characteristics: an internal diameter of 112 nm, a wall thickness of 26 nm, nanotube length of 15 μm, a roughness factor of 1840 points, and an anatase-rutile crystalline structure. In the hybrid bioreactor, 39% IND and 50% ACL and DCL were removed. The biological-photocatalysis sequential system achieved the degradation of up to 90% of the initial concentrations of the three acid pharmaceuticals studied. This approach appears to be a viable alternative for the treatment of these non-biodegradable effluents.

Keywords: persistent acid pharmaceuticals; sequential system; biological-photocatalytic processes; NTF-TiO₂; fixed bed bioreactor



Citation: Cruz-Carrillo, M.J.; Melgoza-Alemán, R.M.; Cuevas-Arteaga, C.; Proal-Nájera, J.B. Removal of Persistent Acid Pharmaceuticals by a Biological-Photocatalytic Sequential Process: Clofibric Acid, Diclofenac, and Indomethacin. *Catalysts* **2022**, *12*, 1488. <https://doi.org/10.3390/catal12111488>

Academic Editor: Meng Li

Received: 21 October 2022

Accepted: 16 November 2022

Published: 21 November 2022

Publisher's Note: MDPI stays neutral with regard to jurisdictional claims in published maps and institutional affiliations.



Copyright: © 2022 by the authors. Licensee MDPI, Basel, Switzerland. This article is an open access article distributed under the terms and conditions of the Creative Commons Attribution (CC BY) license (<https://creativecommons.org/licenses/by/4.0/>).

1. Introduction

Pharmaceutical active compounds (PhACs), many of which are pervasive, recalcitrant, and biologically active substances, have incited growing concern, mainly because no legislation has been established for their discharge into surface water bodies [1,2]. Vast quantities of PhACs are used all over the world and are able to reach the aquatic environment via urinary excretion and the unsuitable disposal of medication. Hence, these compounds have been found in wastewaters and in surface waters, as they are currently not completely eliminated in wastewater treatment plants (WWTPs) [3,4]. Numerous studies have shown that levels of PhACs are high in aquatic environments and that there is a risk of adverse effects on aquatic organisms. Pharmaceuticals have been found in freshwater environments at concentrations above the threshold for pharmacological effects on fish [5,6].

Among PhACs, a group that has recently received a lot of attention due to its persistent occurrence in different water sources is that of analgesic and non-steroidal anti-inflammatory drugs (NSAIDs). This group currently comprises more than one hundred compounds that are widely used around the world. Another important and regularly observed group of PhACs is lipid regulators. Lipid regulators are widely used and are one of the most common PhAC groups, according to consumption and prescriptions [7,8]. Among PhACs, clofibric acid (CLA), diclofenac (DCL), and indomethacin (IND) are commonly

detected in aquatic environments due to their incomplete removal during wastewater treatment processes. As such, these compounds are receiving increasing attention as recalcitrant environmental contaminants [9–12]. For some PhACs, considerably higher removal rates have been achieved through the use of biofilm carriers compared to activated sludge [13,14], suggesting that the further optimization of the biological micropollutant removal processes is within the realm of possibility. Hybrid suspended/attached growth processes combine biofilm carriers and activated sludge into a single treatment procedure. The probability of achieving effective removal using an attached growth biomass is high, as it comprises a diverse bacterial community with aerobic, anoxic, and anaerobic actions [15].

In addition, advanced oxidation processes (AOPs) have been proposed as tertiary treatments for WWTP effluents due to their versatility and ability to increase the biodegradability and detoxification of effluent streams containing polar and hydrophilic chemicals [16]. The principle of AOPs is based on the in situ generation of highly reactive transitory species (i.e., H_2O_2 , $\text{OH}\bullet$, $\text{O}_2^{\bullet-}$, and O_3) for the mineralization of refractory organic compounds [17]. Within the most extensively used AOPs, heterogeneous photocatalysis (HP) occurs. The principle of HP is based on the excitation of a semiconductor (i.e., TiO_2) by light (UV or visible) [18]. Titanium dioxide is a wide-band gap semiconductor that is frequently used in photocatalysis, as it is easily available, stable to photochemical corrosion, cheap, non-toxic, and has excellent photocatalytic activity [19–22].

TiO_2 powders have been used for many years in the area of photocatalysis and their benefits have accelerated progress in the field. Nevertheless, this material has several shortcomings: it is difficult to disperse and to reuse, it is easily agglomerative, it has low light response properties, and, finally, it causes environmental contamination when used inadequately. The introduction of TiO_2 nanotube arrays (NT- TiO_2), a novel form of TiO_2 , has resolved these problems. The structural parameters of NT- TiO_2 , such as its specific surface area, wall thickness, tube length, and crystalline phase, have important effects on the photocatalytic activity of nanotube arrays [23,24]. NT- TiO_2 have been extensively applied for the degradation of various organic microcontaminants, such as azo dyes, phenols, and PhACs, among others [25–29].

The coupling of a biological process to an AOP is applied to treat wastewater containing refractory compounds and to limit the high treatment costs associated with chemical oxidation. In these coupled processes, chemical oxidation can be used as a pre-treatment to decrease toxicity or as a post-treatment for the final cleansing of the wastewater [30]. The measurements of the efficiency of the combined process depend on the purpose of the treatment; however, it is usually necessary to independently optimize each of the two stages, i.e., biological and chemical [31]. To augment the elimination of pharmaceutical products, conventional and alternative wastewater treatment processes and their combinations have been researched [32–34]. Nonetheless, the literature on the elimination of CLA, DCL, and IND using coupled biological–AOP systems is scarce.

Some research has been carried out to study the removal of various pharmaceutical products using biological methods combined with POA. Wilt et al. (2020) [35] used a combined process, i.e., photocatalysis UV/ TiO_2 –biological, to efficiently remove eight out of nine studied compounds (atenolol, atorvastatin, caffeine, carbamazepine, diclofenac, gemfibrozil, fluoxetine, ibuprofen, and naproxen). They determined that the degree of biodegradation following photocatalysis was improved for some drugs (caffeine, diclofenac, gemfibrozil, and ibuprofen) while for others, such as carbamazepine, the approach was ineffective. In 2019, Wang et al. [36] investigated the mineralization of amoxicillin via an intimately coupled photocatalysis (Ag-doped TiO_2) and biodegradation (biofilm) process. The results they obtained using the combined process showed removal rates 40% greater than when using photocatalysis alone, and 65% higher than when using biodegradation alone. The degree of mineralization was around 35% with the combined process, while in the separate processes, it was minimal. Zupanc et al. (2013) [37] studied the removal efficiencies for clofibric acid, ibuprofen, naproxen, ketoprofen, carbamazepine, and diclofenac by two treatment processes: a suspended, activated sludge and moving bed biofilm process

(MBBR) and hydrodynamic cavitation (HC) with the addition of H_2O_2 and UV irradiation. The highest average removals of all the investigated compounds were achieved when the biological treatment (MBBR), HC/ H_2O_2 process, and UV treatment were applied consecutively.

The main objective of this study was to assess the feasibility of a hybrid biological process (i.e., a fixed bed bioreactor and activated sludge) sequenced to a photocatalysis process employing TiO_2 nanotubular films (NTF- TiO_2) for the removal of three acidic PhACs (clofibric acid, diclofenac, and indomethacin).

2. Results and Discussion

2.1. Biological Process

The hybrid bioreactor (HBR) was operated as a hybrid reactor using two processes: activated sludge and adhered biomass supported in biomedia. The HBR bioreactor operated for 86 days (28 cycles). During this period, the dissolved oxygen (DO) level varied in the range of <1 and 5 mg L^{-1} , with a pH of 7.5 ± 0.2 and a temperature inside the reactor of $22^\circ\text{C} \pm 2^\circ\text{C}$.

2.1.1. Biomass Acclimatization

The duration of the HBR acclimatization phase was 46 days (cycle 1 to 7). The acclimation began with a concentration of 2 mg L^{-1} of the PhACs dissolved in methanol (MeOH). During this phase, the removal efficiencies fluctuated between 3% and 17% for the CLA, 8% and 18% for the DCL, and 5 and 15% for the IND. The reaction time was 192 h to 72 h; this could have been the consequence of a non-acclimated biomass and an immature biofilm since biofilms need a long maturation time [38]. Regarding the total organic carbon (TOC) concentration, the removal of TOC was observed to be unstable, as it fluctuated between 20% and 50%. The low removal of TOC during the first days is a normal process in the start-up phase, because the biomass is not acclimated to the removal of PhACs. To consider an acclimatized biomass, 80% PhAC removal was set; however, due to drug recalcitrance, which involves complex structures that bacteria find difficult to degrade, fixed removal efficiencies were not achieved, so it was considered to take as an adaptation criterion the removal of 80% of the TOC. This adaptation was reached in cycle 7. According to the stoichiometric reaction, it was observed that the greatest contribution of carbon was due to MeOH, which acted as a co-substrate, providing an easily degradable carbon source for the bacteria. Table 1 summarizes the HBR's operating parameters during the acclimatization phase.

Table 1. Operating parameters of the HBR bioreactor during the acclimatization phase: cycle, reaction time, TOC concentration, and removal % of TOC, ACL, DCL, and IND.

Cycle	Reaction Time (h)	mg L ⁻¹ TOC Influent	% Removal TOC	% Removal		
				ACL	DCL	IND
1	192	155.57	21.50	18.0	18.8	31.8
2	192	143.43	29.74	4.5	8.4	10.2
3	192	148.52	51.12	6.8	17.3	7.3
4	148	174.24	55.18	11.8	7.4	12.9
5	148	188.15	74.35	17.6	11.9	5.0
6	148	144.44	52.33	2.9	8.1	14.6
7	72	166.15	80.19	3.0	18.2	11.9

2.1.2. Behavior of Biomass and Total Suspended Solids

The biomass was determined as volatile suspended solids in the mixed liquor (MLVSS). Figure 1 shows the evolution of the biomass that oscillated between 1800 and 1300 mg L^{-1} . During the first 40 days of the reactor's operation, a decrease in biomass was observed, causing a loss in bacterial activity, which was a product of the process of the biomass' adaptation to the degradation of the PhACs. To strengthen the biomass, for 12 days (cycle

8 to 11), only MeOH (0.02%) was added as an easily degradable substrate. At 58 days, the amount of biomass gradually increased until reaching 1800 mg L^{-1} . The results showed that there was a sufficient degree of biomass recovery in order to synthesize new cells.

The total suspended solids (TSS) in the HBR effluent decreased from 216 mg L^{-1} to $25 \pm 3 \text{ mg L}^{-1}$ (Figure 1) as a result of the reactor's stabilization. Some authors [39–42] have reported poor sludge settleability and high solids in the effluent when operating at low DO concentrations. In this work, no negative impacts on the sludge's settleability were observed when the reactor operated at DO concentrations $< 1 \text{ mg/L}$. The operating conditions of the reactor favored the growth of bacteria capable of forming favorable flocs for a good settleability and development of biomass.

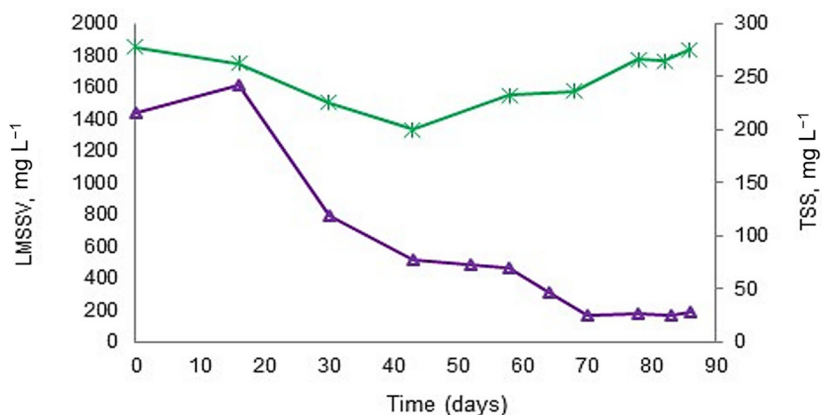


Figure 1. Behavior of biomass (green line with asterisks) and TSS (purple line with triangles).

2.1.3. Total Organic Carbon

After the acclimatization phase, a decrease in TOC removal was observed due to biomass inhibition. As a strategy to strengthen the biomass, the addition of the PhACs was suspended (cycle 8 to 11), adding only MeOH (0.02%) to the HBR. At this phase, the average TOC removal was 79% with reaction times of 72 h. After this recovery phase, the PhACs were again added to the HBR. From this phase (cycle 12 to 28), the removal efficiencies gradually increased up to $90\% \pm 5\%$. The reaction time was optimized from 192 h to 24 h. Figure 2 presents the total organic carbon (TOC) concentration in the influent and effluent and the removal efficiency during all the operation periods of the HBR.

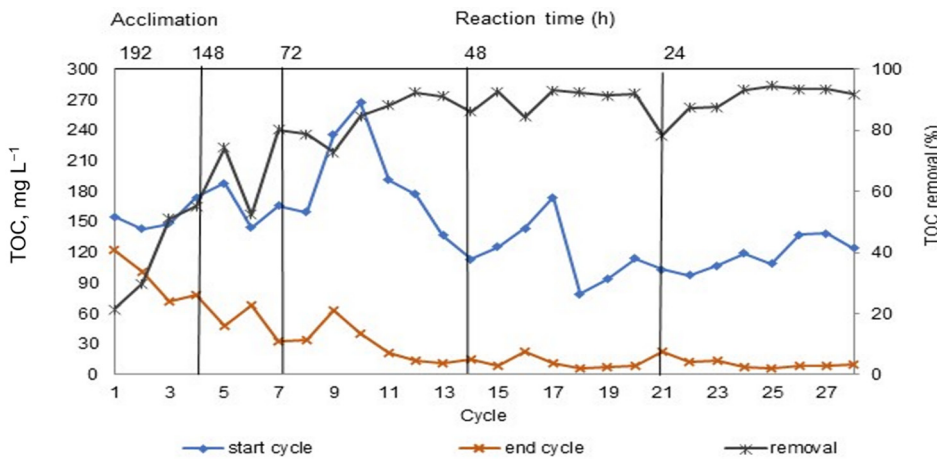


Figure 2. Behavior of influent and effluent TOC concentrations and TOC removal.

2.1.4. PhACs Biodegradation

After the biomass recovery phase, removal efficiencies of 39% were obtained for the IND and 50% for the ACL and DCL. The evolution of the removal efficiencies and reaction

times during the operation of the reactor are presented in Figure 3a–c. The removal of the PhACs investigated in the present study fell into the range reported in [43–45].

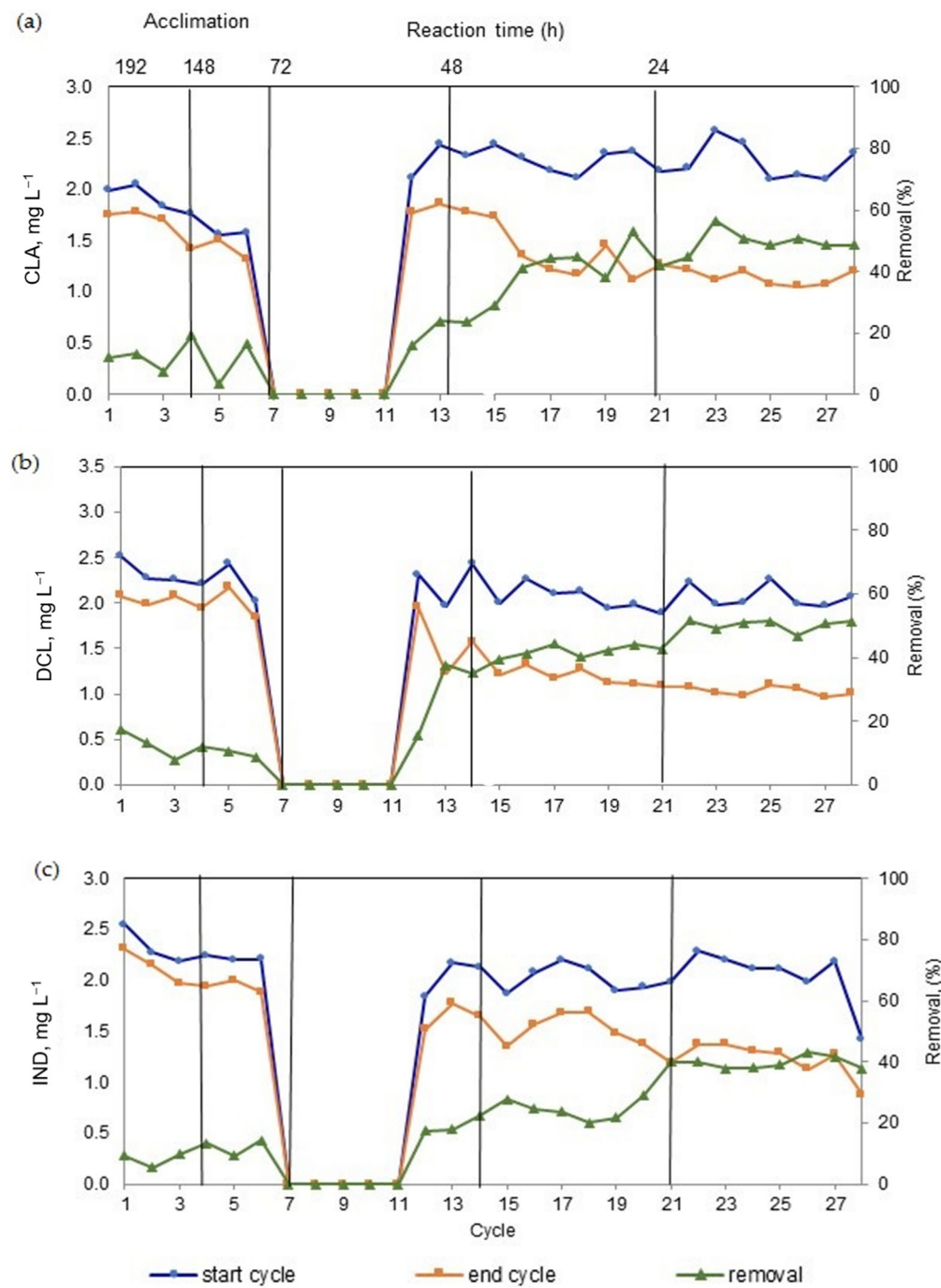


Figure 3. Evolution of the removal efficiencies and reaction times. (a) CLA; (b) DCL; (c) IND.

Some authors attribute high PhAC removal to the substrate and redox gradients within the biofilm, which may induce vastly stratified microbial communities, with microorganisms adapted to easily degradable organic substrates in the outer part of the biofilm and microorganisms adapted to the remaining and hardly degradable organic substrates in the inner part of the biofilm [14,38].

On the other hand, the addition of MeOH as a source of external carbon can lead to the development of a diverse microbial community that favors the growth of nitrifying bacteria associated with the biodegradation and biotransformation of PhACs [15,38,46–48].

2.2. Biological-Photocatalytic Sequential System

Since the fixed efficiencies criterion (80% PhACs removal) was not achieved and, consequently, there were still remnants of the PhACs not removed in the HBR bioreactor, coupling to photocatalysis was performed. To determine the operating conditions of the photocatalysis process, the effluent of the HBR bioreactor was used. The parameters evaluated to determine the optimal operating conditions in the photocatalytic process were the area of the NTF-TiO₂ catalyst, the wavelength of UV radiation (UV-A and UV-C), and pH.

2.2.1. NTF-TiO₂ Catalyst

Some factors that influence the efficiency of photocatalysis using NTF-TiO₂ are the morphology and structure (including the thickness of the tube wall), diameter, and length of the nanotubes [27]. In our study, NTF-TiO₂ with a wall thickness of 26 nm, a length of 65 μ m, and a diameter of 112 nm were used. In comparison with other reported works, they are four times larger with respect to length and up to 12 times larger with respect to diameter [49]. Smith et al. 2009 [50] observed that as the diameter, length, and thickness of the NTF-TiO₂ increase, higher photocatalytic activity is observed. Figure 4 shows some Field Emission Scanning Electron Microscopy (FE-SEM) images of the morphological characteristics. Figure 4a shows the open top view, whereas Figure 4b,c show the cross section of the nanofilm.

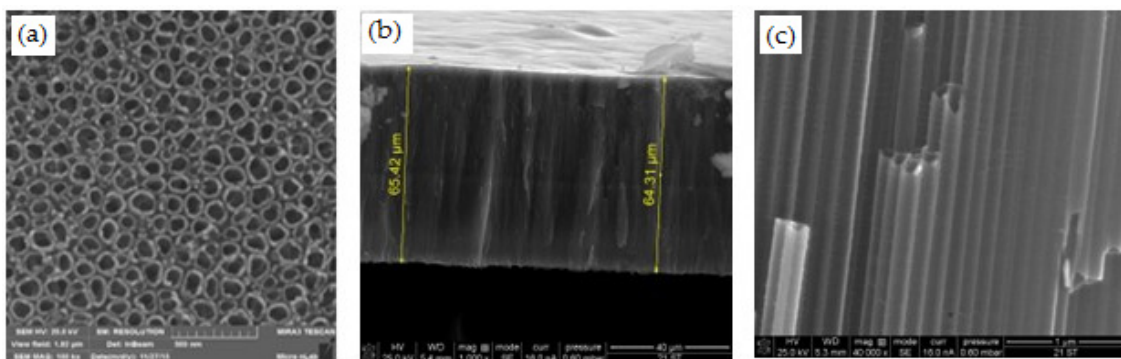


Figure 4. FE-SEM images of the NTF-TiO₂. (a) Top view; (b) and (c) cross sectional views.

With respect to the crystalline structure, Figure 5 presents the X-ray Diffraction (XRD) spectrum of the NTF-TiO₂. The XRD spectrum shows the main presence of anatase (JCPDS Card # 21-1272) in coexistence with rutile phases (JCPDS card # 21-1276), observing a very intensive peak of anatase together with two other medium intensive anatase peaks. From the XRD spectrum, it can be observed that the major peak corresponds to the anatase phase. As reported, the crystalline structure plays an important role in the photoactivity of the NTF-TiO₂; for instance, with the crystalline structure anatase as the major phase in combination with rutile, the best photocatalytic performance was determined, followed by the rutile phase and amorphous structures [51]. In this study, the presence of the anatase phase in a greater proportion was a factor that favored the degradation of the PhACs, which has been reported in studies on the influence of crystal structure on the removal of diverse molecules such as PhACs [52,53], phenols [27], and dyes [25].

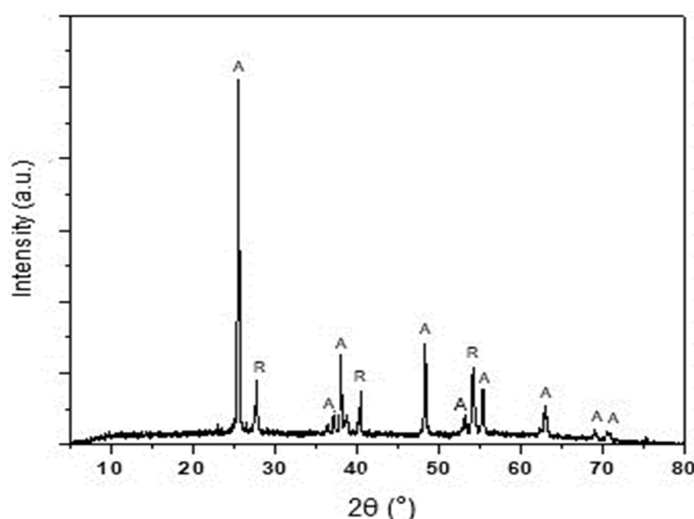


Figure 5. XRD spectrum of the NTF-TiO₂. A (anatase phase); R (rutile phase).

2.2.2. pH Effect

In the photocatalytic process, the generation of hydroxyl radicals is a function of pH. Thus, pH is an important parameter in photocatalytic reactions [54]. In this study, we investigated the effect of pH on photocatalytic performance. The experiments were carried out employing a 4 cm² area of NTF-TiO₂ and UV-A radiation. The studied pH levels were 3.5 ± 0.2 and 7.3 ± 0.2 . After 48 h of reaction, the best performance was evidenced at pH 3.5 with removal efficiencies of 97% for the CLA and 100% for the IND and DCL. In the case of pH 7.3, after 72 h of reaction, the removals were 38%, 61%, and 82% for the CLA, DCL, and IND respectively. This influence of pH on the photodegradation of PhACs, using TiO₂ catalyst, is consistent with that reported by Molinari et al. in 2006 [55]. The previous results may be due to the fact that when working at pH 3.5 and 7.2, on the one hand, the ionization of PhACs is favored, since their pKa are 3.18, 4.10, and 4.50 for CLA, DCL, and IND, respectively, while on the other hand, the isoelectric point (PZC) reported for TiO₂ [17] is in the pH range of 4.5 and 7.0; thus, at pH lower than PZC, the catalyst acquires a positive charge and gradually exerts a electrostatic attraction force towards the ionized species of the PhACs favoring adsorption on the TiO₂ surface for subsequent photocatalytic reactions.

Several authors [50,56,57] have already reported the influence of pH on TiO₂ through the photocatalytic degradation of PhACs and found minimal influence in the near neutral pH range. In our study, as shown in Table 2, the best removal efficiencies were achieved at pH 3.5; however, the average pH of the biological treatment effluents was 7.3 ± 0.2 , so the high removal efficiencies achieved at pH 7.3 are an important finding, since the biological treatment effluent can be treated directly without treatment prior to photocatalysis. On the other hand, there is an advantage of showing that the removal efficiency through a sequenced biological process to photocatalysis in acidic and near neutral pH conditions can be an alternative treatment for wastewaters with different pH conditions. Nevertheless, it is better to evaluate the effect of pH on photodegradation in a way that considers the contaminant properties, the type of photocatalyst, and the effluent to treat.

2.2.3. Effect of the NTF-TiO₂ Area and UV Radiation

Experiments were carried out using a film of NTF-TiO₂ (area 2 cm²) and with two films of NTF-TiO₂ (area 4 cm²), UV-A radiation, and pH 7.5. The results of the biological-photocatalytic sequential system under different operating conditions are presented in Table 2. In the experiments using an area of 2 cm², the degree of photodegradation was 26% for the ACL, 62% for the DCL, and 84% for the IND after 72 h of reaction (Table 2). Whereas when the catalyst area was increased to 4 cm², no changes in photodegradation were observed. The removals were 38%, 61%, and 82% for CLA, DCL, and IND, respectively. Subsequently, experiments with 4 and 8 cm² of NTF-TiO₂ area, applying UV-C radiation,

and at pH 7.4 were carried out. When UV-C radiation and the 4 cm^2 area of NT-TiO₂ were used, an increase in the removal was observed for the three PhACs. The removals were 100%, 77%, and 64% for the CLA, DCL, and IND, respectively. The reaction time was 5 h. When increasing the area of the NTF-TiO₂ to 8 cm^2 under the same conditions of pH and UV radiation, a further removal was favored, reaching 100% degradation for the DCL and IND. The photodegradation times were 5 h for IND and 2 h for DCL. The CLA was photodegraded up to 90% over a reaction time of 3 h (Table 2).

Table 2. Results of the biological–photocatalytic sequential system under different operating conditions.

Experiments	UV-365 nm (UV-A)			UV-254 nm (UV-C)	
	2 cm^2 NTF-TiO ₂		4 cm^2 NTF-TiO ₂	8 cm^2 NTF-TiO ₂	
	pH 7.5	pH 3.5	pH 7.3	pH 7.4	
	RT = 72 h	RT = 48 h	RT = 72 h	RT = 5 h	RT
PhACs					Removal Efficiencies (%)
CLA	26	97	38	100	90 (3 h)
DCL	62	100	61	77	100 (2 h)
IND	84	100	82	64	100 (5 h)

RT = reaction time.

The experiments carried out without the nanotubes (control photolytic experiments) were performed only at a pH of 7.3, since it is the average pH of the biological treatment effluent. The removal efficiencies were 3%, 5%, and 25% for CLA, DCL, and IND, respectively, after 4 h of reaction and UV-C radiation (254 nm), so the effect of photolysis alone is not sufficient to achieve the total removal of the PhACs.

2.3. Kinetic Study

The reaction kinetics of the photocatalytic process were determined. The concentration was determined by UV-Vis spectroscopy and HPLC. The reaction kinetics of the PhAC mixture were determined by applying UV-A and UV-C radiation, pH 7.4, and areas of 4 cm^2 and 8 cm^2 . The NTF-TiO₂ films were first immersed in the PhACs mixture (effluent of HBR bioreactor) in the dark for 30 min to reach the adsorption equilibrium. Then, the light was turned on ($t = 0\text{ min}$) and photocatalytic degradation occurred. Figure 6a shows the absorption spectrum of the CLA, DCL, and IND mixtures obtained from the monitoring of the reaction kinetics using UV-Vis, an area of 8 cm^2 of NTF-TiO₂, UV-C radiation, and pH 7.4. Figure 6b shows the absorption spectra of CLA, DCL, and IND.

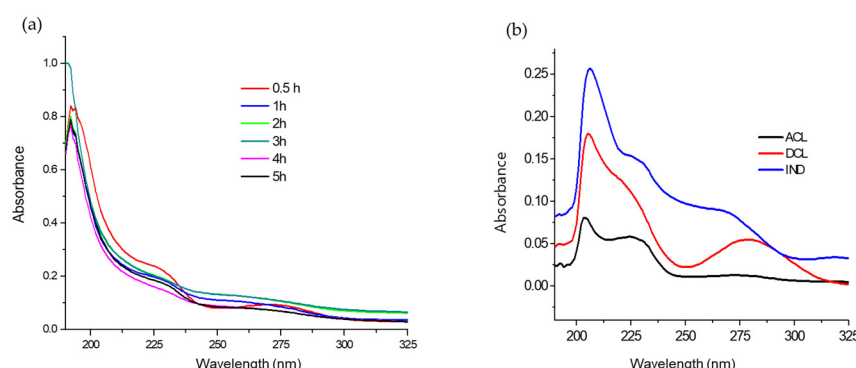


Figure 6. (a) Monitoring of reaction kinetics of CLA, DCL, and IND mixture, using area of 8 cm^2 of NTF-TiO₂, UV-C radiation, and pH 7.4 (b) Absorption spectrum of CLA, DCL, and IND.

Figure 7 shows the results of the photocatalytic degradation of the CLA, DCL, and IND mixtures, which follow a first order reaction model. Figure 7a shows the degradation kinetics using UV-A radiation and a 4 cm^2 area of the NTF-TiO₂, Figure 7b shows the degradation kinetics using UV-C radiation and a 4 cm^2 area of the NTF-TiO₂, and Figure 7c shows the degradation kinetics using UV-C radiation and an area of 8 cm^2 of NTF-TiO₂. The results in Figure 7 confirm the data presented in Table 2.

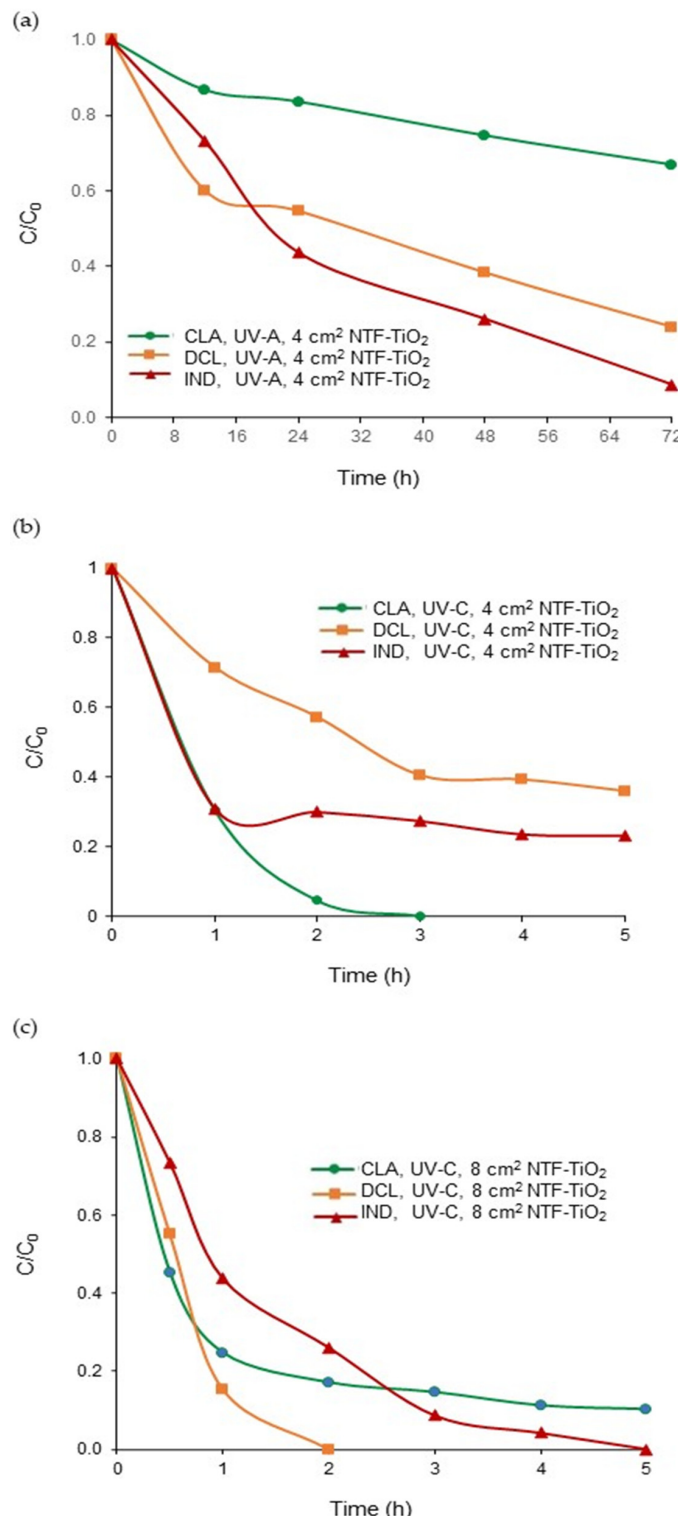


Figure 7. Photocatalytic degradations of CLA, DCL, and IND mixture. (a) UV-A radiation and 4 cm^2 of NTF-TiO₂; (b) UV-C radiation and 4 cm^2 of NTF-TiO₂; (c) UV-C radiation and 8 cm^2 of NTF-TiO₂.

The concentrations of the PhACs mixture, the results of the kinetic constants, the correlation coefficient, and the percentage removal (%) of the kinetic study of the biological-photocatalysis sequential system are summarized in Table 3. Based on the results, it can be observed that the photoactivity was the lowest—with rate constants of 0.0042, 0.0091, and 0.0121 for the CLA, DCL, and IND, respectively, and with removals of 33.27, 76.07, and 83.97% after 72 h—when UV-A radiation was used. By increasing the area of NTF-TiO₂ and applying UV-C radiation, the photoactivity increased significantly, showing better results when using an area of 8 cm² with the rate constants of 0.1304, 0.4855, and 0.1871 for CLA, DCL, and IND, respectively, and removals of 89.95% for CLA and 100% for the DCL and IND after 5 h, 2 h, and 4 h, respectively. Figure 8 shows the comparison of the achieved rate constants (Figure 8a) and removals (Figure 8b).

Table 3. Kinetic constants, correlation coefficients, and PhACs removal percentage (%) from kinetic study of the biological-photocatalysis sequential system.

PhACs	mg L ⁻¹	UV-A/4 cm ² K (h ⁻¹)	Removal (%)	mg L ⁻¹	UV-C/4 cm ² K (h ⁻¹)	Removal (%)	mg L ⁻¹	UV-C/8 cm ² K (h ⁻¹)	Removal (%)
CLA	1.93	0.0042 (R ² = 0.9358)	33.27	1.75	0.3255 (R ² = 0.8299)	99.88	2.40	0.1304 (R ² = 0.5651)	89.95
DCL	1.88	0.0091 (R ² = 0.8444)	76.07	1.27	0.1240 (R ² = 0.8698)	76.80	2.57	0.4855 (R ² = 0.8588)	100
IND	2.63	0.0121 (R ² = 0.9156)	83.97	2.69	0.1167 (R ² = 0.5311)	64.10	1.24	0.1871 (R ² = 0.8413)	100

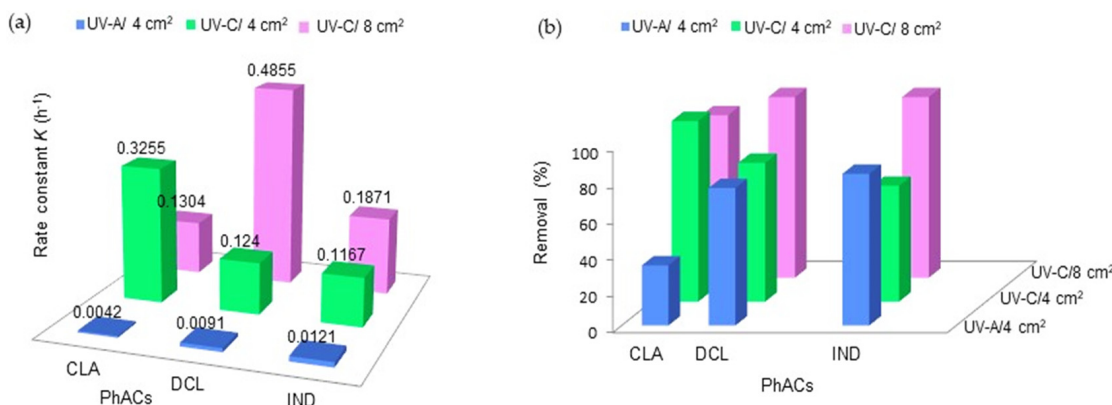


Figure 8. Comparison of rate constants (a) and the achieved removals (b) from kinetic study of the biologica-photocatalysis sequential system.

The results presented in Figure 8 correspond to the performance of NTF-TiO₂ as a catalyst when irradiated with UV radiation (being initially in their basal state), wherein they absorb the energy of the light and thereby form an excited state that can lead to photochemical reactions, such as the breaking of bonds [58]. The energy at a wavelength of 254 nm (UV-C) is greater than at a UV-A wavelength, which favors photodegradation. In addition, the absorption spectrum of the PhACs (Figure 6b) shows maximum absorption in the UV-C region. These results are consistent with previous studies, where the photodegradation of organic molecules (PhACs and azo-type dyes) was investigated using UV irradiation at various wavelengths [58–62]. With respect to the area of NTF-TiO₂, the results showed that increasing the area of the nanofilms increased removal due to a larger quantity of nanotubes; therefore, the ability to adsorb light and generate photo-induced electron-hole pairs inactive sites was greater, which led to an increase in photodegradation efficiency.

3. Materials and Methods

3.1. Reagents

PhACs of standard grade $\geq 98\%$ purity, namely, clofibrate acid (CLA), diclofenac (DCL), and indomethacin (IND); substances of nutrient mineral medium [63]; ethylene glycol; and NH₄F were acquired from Sigma Aldrich. Figure 9 shows the chemical structures of the utilized pharmaceuticals.

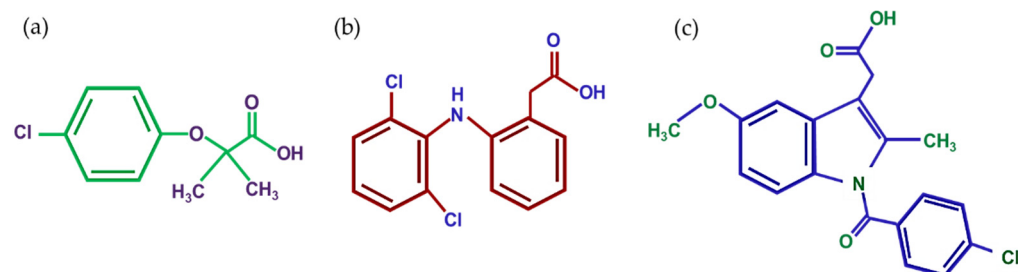


Figure 9. Chemical structures: (a) clofibrate acid, (b) diclofenac, and (c) indomethacin.

3.2. Hybrid Biological Process

For the inoculation of the HBR, the activated sludge was obtained from the wastewater treatment plant ECCACIV, located in Jiutepec-Morelos, México.

3.2.1. Biomass Acclimatization and Operation Strategy

The biomass was acclimatized to the pharmaceuticals by feeding nutrient mineral medium (Table 4) and CLA, DCL, and IND dissolved in MeOH. Inlet concentrations of PhACs were about 2 mg L⁻¹. The adaptation of microorganisms for treating wastewater was carried out with variable reaction cycles to reach the acclimatization of biomass for degradation of PhACs using the criteria-fixed efficiencies [64], which consisted of allowing biomass to adapt to degradation of 80% of PhACs. The experiments were performed in batches. These batch experiments were carried out in 4 stages: filling, reaction, sedimentation, and emptying.

Table 4. Composition of nutrient mineral medium.

Substances	mg L ⁻¹
K ₂ HPO ₄	65.25
Na ₂ HPO ₄ ·2H ₂ O	100.2
KH ₂ PO ₄	25.5
NH ₄ Cl	7.5
MgSO ₄ ·7H ₂ O	22.5
CaCl ₂ ·2H ₂ O	27.5
FeCl ₃ ·6H ₂ O	0.25
H ₃ BO ₃	0.06
MnSO ₄ ·H ₂ O	0.04
ZnSO ₄ ·7H ₂ O	0.04
(NH ₄) ₆ Mo ₇ O ₂₄	0.03
EDTA	0.1

3.2.2. Experimental System (HBR Bioreactor)

The experimental set up consisted of an acrylic reactor with a total volume of 6.5 L and a useful volume of 4 L. For the control of loading, recirculating, and discharge, two peristaltic pumps were used (Master Flex, Cole Palmer, Vernon Hills, Chicago, IL, USA).

The air inside the reactor was distributed from the bottom of the reactor through a porous diffuser with an air pump. For HBR configurations, 50% of the useful volume of reactor was filled with high-density polypropylene plastic carriers (biomedia AMB, DYNAMIC AQUA SCIENCE, Kirkland, AZ, USA).

The control parameters of the HBR were the concentrations of biomass measured as MLVSS, TSS, TOC and PhACs, DO, pH, and temperature.

3.3. Photocatalytic System

The effect of pH, area of NTF-TiO₂, and UV radiation, on the photocatalytic performance of NTF-TiO₂ were investigated.

3.3.1. TiO₂ Nanostructures Films

NTF-TiO₂ were synthesized by the electrochemical anodization technique. Electrochemical anodization experiments were performed in a nonaqueous electrolytic solution of ethylene glycol (3 vol% H₂O) + 0.25 wt% NH₄F. The anodization process lasted 11.5 h, maintaining a constant voltage of 60 V at room temperature. After anodization, the samples were rinsed with deionized water and dried in a N₂ stream. The total area anodized was 2 cm². The morphological and structural characterization of NTF-TiO₂ was carried out by means of FE-SEM and an XRD.

3.3.2. Biological-Photocatalytic Sequential System

Photocatalysis experiments were performed in a glass cell with a water recirculation jacket to control the temperature, using 60 mL of the effluent from the HBR, which contained CLA, DCL, and IND not removed by the biological system. The sample for photocatalysis was taken immediately after finishing the cycle of the biological process.

The glass cell was irradiated with UV-A (365 nm) or UV-C (254 nm) lamps and in dark conditions. For the optimization of the process, experiments were carried out with two different pH values: 7.3 ± 0.2 and 3.5 ± 0.2, employing 2, 4, and 8 cm² areas of NTF-TiO₂. Once the optimal conditions of operation were determined, reaction kinetics were performed. The scheme of biological-photocatalytic sequential system is shown in Figure 10.

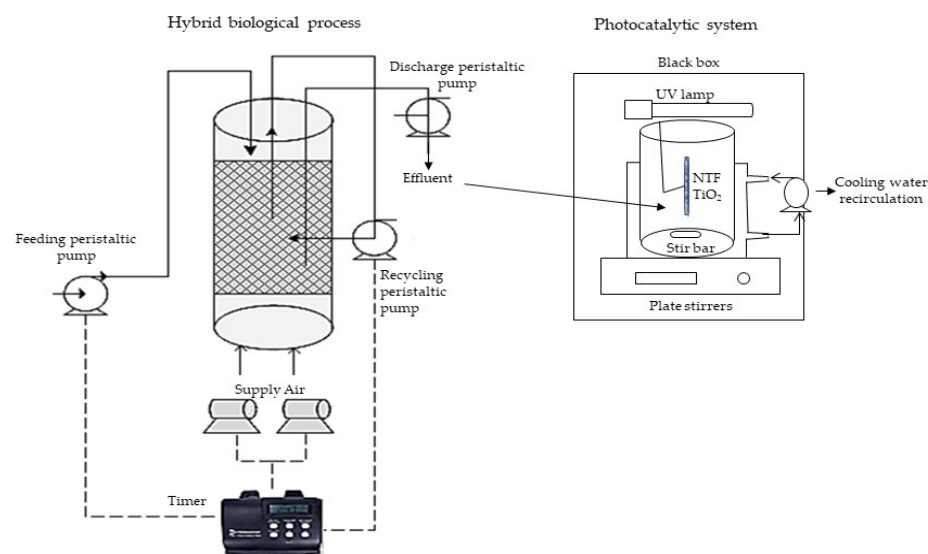


Figure 10. Biological-photocatalytic sequential system.

3.3.3. Analytical Methods

PhACs concentrations were determined by high performance liquid chromatograph HPLC 1100 (Agilent, Mexico City, Mexico), which was equipped with Zorbax Eclipse XDB C-18 (250 mm × 4.6 mm × 5 µm) column (LEACSA SA de CV, Mexico City, Mexico) at

35 °C and a UV detector with a wavelength of 230 nm. The mobile phase, with a flow rate of 0.8 mL/min, was composed of acetonitrile:1% acetic acid water mixture with a volumetric ratio of 65:35. The volume of the injected sample was 10 µL. The samples to determine the concentration of the PhACs were previously centrifuged at 3000 rpm for 15 min and then filtered through a membrane of 45 µm. PhACs absorption spectra were determined by a spectrophotometer UV-VIS Lambda 25, Perkin Elmer (Perkin Elmer de México, Mexico City, Mexico). TOC of samples was analyzed using a TOC analyzer (Torch TELEDYNE Tekmar, MAC Analítica SA de CV, Estado de México, Mexico). Samples were centrifuged at 3000 rpm for 15 min, and then they were filtered through fiberglass paper. The control parameters—DO, temperature, and pH—were determined by APHA Methods 2005 [65].

3.4. Kinetic Study

Kinetic analysis was performed considering a first order reaction (Equation (1)) [66]. The rate constant (k) of the photocatalytic reaction for the PhACs degradation process was determined through Equation (1).

$$\ln(C/C_0) = -k \times t \quad (1)$$

where C corresponds to PhACs concentration at time t , C_0 represents the PhACs initial concentration of the sample, and t is the time at which the sample was taken.

The kinetic curves for PhACs degradation were obtained by a non-linear relationship (C/C_0 vs. t) for each treatment [67].

4. Conclusions

In this study, a biological process utilizing a bioreactor (HBR) sequenced to perform photocatalysis using NTF-TiO₂ for the degradation of CLA, DCL, and IND was optimized.

In the hybrid bioreactor (HBR), the overall removal for IND was 39%, whereas for CLA and DCL the overall removals were 50% over a reaction time of 24 h. The degradation of organic carbon measured as TOC was 92%.

In the biological-photocatalysis sequential system, the overall removal efficiency for the CLA was 90%, whereas for DCL and the IND it was 100% (below the LOD) after 29 h of treatment (24 h of biological process and 5 h of photocatalysis).

It was shown that the photocatalytic degradation reaction of PhACs follows a first-order kinetics pattern, which was dependent on the UV radiation and the area of NTF-TiO₂. The optimal operating parameters were applying UV-C radiation and using 8 cm² of NTF-TiO₂.

The results indicated that the biological-photocatalysis sequential system is a promising method for treating water contaminated with CLA, DCL, and IND.

Author Contributions: Conceptualization, R.M.M.-A.; methodology, M.J.C.-C., R.M.M.-A., C.C.-A. and J.B.P.-N.; formal analysis, M.J.C.-C.; investigation, M.J.C.-C.; resources, M.J.C.-C. and C.C.-A.; data curation, M.J.C.-C., R.M.M.-A., C.C.-A. and J.B.P.-N., writing—original draft preparation, M.J.C.-C.; writing—review and editing, M.J.C.-C., R.M.M.-A., C.C.-A. and J.B.P.-N.; visualization, R.M.M.-A.; supervision, R.M.M.-A.; project administration, R.M.M.-A., C.C.-A. and J.B.P.-N.; funding acquisition, M.J.C.-C., R.M.M.-A., C.C.-A. and J.B.P.-N. All authors have read and agreed to the published version of the manuscript.

Funding: This research received no external funding.

Data Availability Statement: Data are contained within the article.

Acknowledgments: We thank the Facultad de Ciencias Químicas e Ingeniería of Universidad Autónoma del Estado de Morelos (UAEMorelos) and Centro de Investigación en Ingenierías (UAEMorelos) for their help with accomplishing the experiments. We also thank the National Science and Technology Council of Mexico (CONACYT) for the scholarship granted to the first author.

Conflicts of Interest: The authors declare no conflict of interest.

References

- Verlicchi, P.; Al Aukidy, M.; Zambello, E. Occurrence of Pharmaceutical Compounds in Urban Wastewater: Removal, Mass Load and Environmental Risk after a Secondary Treatment—A Review. *Sci. Total Environ.* **2012**, *429*, 123–155. [CrossRef] [PubMed]
- Mendoza, A.; Aceña, J.; Pérez, S.; López de Alda, M.; Barceló, D.; Gil, A.; Valcárcel, Y. Pharmaceuticals and Iodinated Contrast Media in a Hospital Wastewater: A Case Study to Analyse Their Presence and Characterise Their Environmental Risk and Hazard. *Environ. Res.* **2015**, *140*, 225–241. [CrossRef] [PubMed]
- Boix, C.; Ibáñez, M.; Sancho, J.V.; Parsons, J.R.; Voogt, P.d.; Hernández, F. Biotransformation of Pharmaceuticals in Surface Water and during Waste Water Treatment: Identification and Occurrence of Transformation Products. *J. Hazard. Mater.* **2016**, *302*, 175–187. [CrossRef]
- Chonova, T.; Keck, F.; Labanowski, J.; Montuelle, B. Science of the Total Environment Separate Treatment of Hospital and Urban Wastewaters: A Real Scale Comparison of Effluents and Their Effect on Microbial Communities. *Sci. Total Environ.* **2016**, *542*, 965–975. [CrossRef]
- Grabicova, K.; Lindberg, R.H.; Östman, M.; Grbic, R.; Randak, T.; Joakim Larsson, D.G.; Fick, J. Tissue-Specific Bioconcentration of Antidepressants in Fish Exposed to Effluent from a Municipal Sewage Treatment Plant. *Sci. Total Environ.* **2014**, *488–489*, 46–50. [CrossRef] [PubMed]
- Ejhed, H.; Fång, J.; Hansen, K.; Graae, L.; Rahmberg, M.; Magnér, J.; Dorgeloh, E.; Plaza, G. The Effect of Hydraulic Retention Time in Onsite Wastewater Treatment and Removal of Pharmaceuticals, Hormones and Phenolic Utility Substances. *Sci. Total Environ.* **2018**, *618*, 250–261. [CrossRef] [PubMed]
- Nikolaou, A.; Meric, S.; Fatta, D. Occurrence Patterns of Pharmaceuticals in Water and Wastewater Environments. *Anal. Bioanal. Chem.* **2007**, *387*, 1225–1234. [CrossRef]
- Feng, L.; van Hullebusch, E.D.; Rodrigo, M.A.; Esposito, G.; Oturan, M.A. Removal of Residual Anti-Inflammatory and Analgesic Pharmaceuticals from Aqueous Systems by Electrochemical Advanced Oxidation Processes. A Review. *Chem. Eng. J.* **2013**, *228*, 944–964. [CrossRef]
- Dordio, A.v.; Duarte, C.; Barreiros, M.; Carvalho, A.J.P.; Pinto, A.P.; Teixeira, C. Bioresource Technology Toxicity and Removal Efficiency of Pharmaceutical Metabolite Clofibric Acid by *Typha* spp.—Potential Use for Phytoremediation? *Bioresour. Technol.* **2009**, *100*, 1156–1161. [CrossRef]
- Basha, S.; Keane, D.; Morrissey, A.; Nolan, K.; Oelgemöller, M.; Tobin, J. Studies on the Adsorption and Kinetics of Photodegradation of Pharmaceutical Compound, Indomethacin Using Novel Photocatalytic Adsorbents (IPCAS). *Ind. Eng. Chem. Res.* **2010**, *49*, 11302–11309. [CrossRef]
- Kim, I.; Yamashita, N.; Tanaka, H. Chemosphere Photodegradation of Pharmaceuticals and Personal Care Products during UV and UV/H₂O₂ Treatments. *Chemosphere* **2009**, *77*, 518–525. [CrossRef]
- Zhao, Y.; Kuang, J.; Zhang, S.; Li, X.; Wang, B.; Huang, J.; Deng, S.; Wang, Y.; Yu, G. Ozonation of Indomethacin: Kinetics, Mechanisms and Toxicity. *J. Hazard. Mater.* **2017**, *323*, 460–470. [CrossRef]
- Yu, T.H.; Lin, A.Y.C.; Lateef, S.K.; Lin, C.F.; Yang, P.Y. Removal of Antibiotics and Non-Steroidal Anti-Inflammatory Drugs by Extended Sludge Age Biological Process. *Chemosphere* **2009**, *77*, 175–181. [CrossRef] [PubMed]
- Falàs, P.; Baillon-Dhumez, A.; Andersen, H.R.; Ledin, A.; La Cour Jansen, J. Suspended Biofilm Carrier and Activated Sludge Removal of Acidic Pharmaceuticals. *Water Res.* **2012**, *46*, 1167–1175. [CrossRef] [PubMed]
- Arya, V.; Philip, L.; Murty Bhallamudi, S. Performance of Suspended and Attached Growth Bioreactors for the Removal of Cationic and Anionic Pharmaceuticals. *Chem. Eng. J.* **2016**, *284*, 1295–1307. [CrossRef]
- Prieto-Rodríguez, L.; Oller, I.; Klamerth, N.; Agüera, A.; Rodríguez, E.M.; Malato, S. Application of Solar AOPs and Ozonation for Elimination of Micropollutants in Municipal Wastewater Treatment Plant Effluents. *Water Res.* **2013**, *47*, 1521–1528. [CrossRef]
- Chong, M.N.; Jin, B.; Chow, C.W.; Saint, C. Recent Developments in Photocatalytic Water Treatment Technology: A Review. *Water Res.* **2010**, *44*, 2997–3027. [CrossRef]
- Andronic, L.; Enesca, A.; Cazan, C.; Visa, M. TiO₂-Active Carbon Composites for Wastewater Photocatalysis. *J. Solgel. Sci. Technol.* **2014**, *71*, 396–405. [CrossRef]
- Sakkas, V.A.; Calza, P.; Medana, C.; Villioti, A.E.; Baiocchi, C.; Pelizzetti, E.; Albanis, T. Heterogeneous Photocatalytic Degradation of the Pharmaceutical Agent Salbutamol in Aqueous Titanium Dioxide Suspensions. *Appl. Catal. B* **2007**, *77*, 135–144. [CrossRef]
- Hu, L.; Flanders, P.M.; Miller, P.L.; Strathmann, T.J. Oxidation of Sulfamethoxazole and Related Antimicrobial Agents by TiO₂ Photocatalysis. *Water Res.* **2007**, *41*, 2612–2626. [CrossRef] [PubMed]
- Wang, J.; Yang, C.; Wang, C.; Han, W.; Zhu, W. Photolytic and Photocatalytic Degradation of Micro Pollutants in a Tubular Reactor and the Reaction Kinetic Models. *Sep. Purif. Technol.* **2014**, *122*, 105–111. [CrossRef]
- Dai, J.; Yang, J.; Wang, X.; Zhang, L.; Li, Y. Enhanced Visible-Light Photocatalytic Activity for Selective Oxidation of Amines into Imines over TiO₂(B)/Anatase Mixed-Phase Nanowires. *Appl. Surf. Sci.* **2015**, *349*, 343–352. [CrossRef]
- Nakata, K.; Ochiai, T.; Murakami, T.; Fujishima, A. Photoenergy Conversion with TiO₂ photocatalysis: New Materials and Recent Applications. *Electrochim. Acta* **2012**, *84*, 103–111. [CrossRef]
- Zhou, Q.; Fang, Z.; Li, J.; Wang, M. Applications of TiO₂ Nanotube Arrays in Environmental and Energy Fields: A Review. *Microporous Mesoporous Mater.* **2015**, *202*, 22–35. [CrossRef]
- Lai, Y.; Sun, L.; Chen, Y.; Zhuang, H.; Lin, C.; Chin, J.W. Effects of the Structure of TiO₂ Nanotube Array on Ti Substrate on Its Photocatalytic Activity. *J. Electrochem. Soc.* **2006**, *153*, D123. [CrossRef]

26. Zhuang, H.; Lin, C. Some Critical Structure Factors of Titanium Oxide Nanotube Array in Its Photocatalytic Activity. *Environ. Sci. Technol.* **2007**, *41*, 4735–4740. [\[CrossRef\]](#)
27. Liang, H.; Li, X. Effects of Structure of Anodic TiO₂ Nanotube Arrays on Photocatalytic Activity for the Degradation of 2,3-Dichlorophenol in Aqueous Solution. *J. Hazard. Mater.* **2009**, *162*, 1415–1422. [\[CrossRef\]](#) [\[PubMed\]](#)
28. Camposeco, R.; Castillo, S.; Navarrete, J.; Gomez, R. Synthesis, Characterization and Photocatalytic Activity of TiO₂ nanostructures: Nanotubes, Nanofibers, Nanowires and Nanoparticles. *Catal. Today* **2016**, *266*, 90–101. [\[CrossRef\]](#)
29. Marien, C.B.D.; Cottineau, T.; Robert, D.; Drogui, P. Applied Catalysis B: Environmental TiO₂ Nanotube Arrays: Influence of Tube Length on the Photocatalytic Degradation of Paraquat. *Appl. Catal. B* **2016**, *194*, 1–6. [\[CrossRef\]](#)
30. Laera, G.; Chong, M.N.; Jin, B.; Lopez, A. An Integrated MBR-TiO₂ Photocatalysis Process for the Removal of Carbamazepine from Simulated Pharmaceutical Industrial Effluent. *Bioresour. Technol.* **2011**, *102*, 7012–7015. [\[CrossRef\]](#)
31. Oller, I.; Malato, S.; Sánchez-Pérez, J.A. Combination of Advanced Oxidation Processes and Biological Treatments for Wastewater Decontamination—A Review. *Sci. Total Environ.* **2011**, *409*, 4141–4166. [\[CrossRef\]](#) [\[PubMed\]](#)
32. Leyva-Díaz, J.C.; López-López, C.; Martín-Pascual, J.; Muñío, M.M.; Poyatos, J.M. Kinetic Study of the Combined Processes of a Membrane Bioreactor and a Hybrid Moving Bed Biofilm Reactor-Membrane Bioreactor with Advanced Oxidation Processes as a Post-Treatment Stage for Wastewater Treatment. *Chem. Eng. Process. Process Intensif.* **2015**, *91*, 57–66. [\[CrossRef\]](#)
33. Lester, Y.; Aga, D.S.; Love, N.G.; Singh, R.R.; Morrissey, I.; Linden, K.G. Integrative Advanced Oxidation and Biofiltration for Treating Pharmaceuticals in Wastewater. *Water Environ. Res.* **2016**, *88*, 1985–1993. [\[CrossRef\]](#)
34. Ganzenko, O.; Trellu, C.; Papirio, S.; Oturan, N.; Huguenot, D.; van Hullebusch, E.D.; Esposito, G.; Oturan, M.A. Bioelectro-Fenton: Evaluation of a Combined Biological—Advanced Oxidation Treatment for Pharmaceutical Wastewater. *Environ. Sci. Pollut. Res.* **2018**, *25*, 20283–20292. [\[CrossRef\]](#) [\[PubMed\]](#)
35. De Wilt, A.; Arlos, M.J.; Servos, M.R.; Rijnaarts, H.H.M.; Langenhoff, A.A.M.; Parker, W.J. Improved Biodegradation of Pharmaceuticals after Mild Photocatalytic Pretreatment. *Water Environ. J.* **2020**, *34*, 704–714. [\[CrossRef\]](#)
36. Wang, Y.; Chen, C.; Zhou, D.; Xiong, H.; Zhou, Y.; Dong, S.; Rittmann, B.E. Eliminating Partial-Transformation Products and Mitigating Residual Toxicity of Amoxicillin through Intimately Coupled Photocatalysis and Biodegradation. *Chemosphere* **2019**, *237*, 124491. [\[CrossRef\]](#) [\[PubMed\]](#)
37. Zupanc, M.; Kosjek, T.; Petkovšek, M.; Dular, M.; Kompare, B.; Širok, B.; Blažeka, Ž.; Heath, E. Removal of Pharmaceuticals from Wastewater by Biological Processes, Hydrodynamic Cavitation and UV Treatment. *Ultrason. Sonochem.* **2013**, *20*, 1104–1112. [\[CrossRef\]](#) [\[PubMed\]](#)
38. De la Torre, T.; Alonso, E.; Santos, J.L.; Rodríguez, C.; Gómez, M.A.; Malfaito, J.J. Trace Organics Removal Using Three Membrane Bioreactor Configurations: MBR, IFAS-MBR and MBMBR. *Water Sci. Technol.* **2015**, *71*, 761–768. [\[CrossRef\]](#)
39. Zeng, A.P.; Deckwer, W.D. Bioreaction Techniques under Microaerobic Conditions: From Molecular Level to Pilot Plant Reactors. *Chem. Eng. Sci.* **1996**, *51*, 2305–2314. [\[CrossRef\]](#)
40. Chu, L.; Zhang, X.; Yang, F.; Li, X. Treatment of Domestic Wastewater by Using a Microaerobic Membrane Bioreactor. *Desalination* **2006**, *189*, 181–192. [\[CrossRef\]](#)
41. Martins, A.M.P.; Heijnen, J.J.; Van Loosdrecht, M.C.M. Effect of Dissolved Oxygen Concentration on Sludge Settleability. *Appl. Microbiol. Biotechnol.* **2003**, *62*, 586–593. [\[CrossRef\]](#)
42. Stadler, L.B.; Su, L.; Moline, C.J.; Ernstoff, A.S.; Aga, D.S.; Love, N.G. Effect of Redox Conditions on Pharmaceutical Loss during Biological Wastewater Treatment Using Sequencing Batch Reactors. *J. Hazard. Mater.* **2015**, *282*, 106–115. [\[CrossRef\]](#) [\[PubMed\]](#)
43. Bo, L.; Urase, T.; Wang, X. Biodegradation of Trace Pharmaceutical Substances in Wastewater by a Membrane Bioreactor. *Front. Environ. Sci. Eng. China* **2009**, *3*, 236–240. [\[CrossRef\]](#)
44. Xue, W.; Wu, C.; Xiao, K.; Huang, X.; Zhou, H. Elimination and Fate of Selected Micro-Organic Pollutants in a Full-Scale Anaerobic/Anoxic/Aerobic Process Combined with Membrane Bioreactor for Municipal Wastewater Reclamation. *Water Res.* **2010**, *44*, 5999–6010. [\[CrossRef\]](#) [\[PubMed\]](#)
45. Casas, M.E.; Chhetri, R.K.; Ooi, G.; Hansen, K.M.S.; Litty, K.; Christensson, M.; Kragelund, C.; Andersen, H.R.; Bester, K. Biodegradation of Pharmaceuticals in Hospital Wastewater by Staged Moving Bed Biofilm Reactors (MBBR). *Water Res.* **2015**, *83*, 293–302. [\[CrossRef\]](#) [\[PubMed\]](#)
46. Krkosek, W.H.; Payne, S.J.; Gagnon, G.A. Removal of Acidic Pharmaceuticals within a Nitrifying Recirculating Biofilter. *J. Hazard. Mater.* **2014**, *273*, 85–93. [\[CrossRef\]](#) [\[PubMed\]](#)
47. Stadler, L.B.; Love, N.G. Impact of Microbial Physiology and Microbial Community Structure on Pharmaceutical Fate Driven by Dissolved Oxygen Concentration in Nitrifying Bioreactors. *Water Res.* **2016**, *104*, 189–199. [\[CrossRef\]](#)
48. Torresi, E.; Casas, M.E.; Polesel, F.; Plósz, B.G.; Christensson, M.; Bester, K. Impact of External Carbon Dose on the Removal of Micropollutants Using Methanol and Ethanol in post-denitrifying Moving Bed Biofilm Reactors. *Water Res.* **2017**, *108*, 95–105. [\[CrossRef\]](#)
49. Zhang, A.; Zhou, M.; Han, L.; Zhou, Q. The Combination of Rotating Disk Photocatalytic Reactor and TiO₂ Nanotube Arrays for Environmental Pollutants Removal. *J. Hazard. Mater.* **2011**, *186*, 1374–1383. [\[CrossRef\]](#)
50. Smith, Y.R.; Kar, A.; Subramanian, V.R. Kinetics, Catalysis, and Reaction Engineering Investigation of Physicochemical Parameters That Influence Photocatalytic Degradation of Methyl Orange over TiO₂ Nanotubes. *Ind. Eng. Chem. Res.* **2009**, *48*, 10268–10276. [\[CrossRef\]](#)

51. Macak, J.M.; Zlamal, M.; Krysa, J.; Schmuki, P. Self-Organized TiO₂ Nanotube Layers as Highly Efficient Photocatalysts. *Small* **2007**, *3*, 300–304. [CrossRef]
52. Nie, X.; Chen, J.; Li, G.; Shi, H.; Zhao, H.; Wong, P.K.; An, T. Synthesis and Characterization of TiO₂ Nanotube Photoanode and Its Application in Photoelectrocatalytic Degradation of Model Environmental Pharmaceuticals. *J. Chem. Technol. Biotechnol.* **2013**, *88*, 1488–1497. [CrossRef]
53. Ye, Y.; Feng, Y.; Bruning, H.; Yntema, D.; Rijnarts, H.H.M. Applied Catalysis B: Environmental Photocatalytic Degradation of Metoprolol by TiO₂ Nanotube Arrays and UV-LED: Effects of Catalyst Properties, Operational Parameters, Commonly Present Water Constituents, and Photo-Induced Reactive Species. *Appl. Catal. B Environ.* **2018**, *220*, 171–181. [CrossRef]
54. Rezaei, M.; Royaei, S.J.; Jafarikojour, M. Performance Evaluation of a Continuous Flow Photocatalytic Reactor for Wastewater Treatment. *Environ. Sci. Pollut. Res.* **2014**, *21*, 12505–12517. [CrossRef]
55. Molinari, R.; Pirillo, F.; Loddo, V.; Palmisano, L. Heterogeneous Photocatalytic Degradation of Pharmaceuticals in Water by Using Polycrystalline TiO₂ and a Nanofiltration Membrane Reactor. *Catal. Today* **2006**, *118*, 205–213. [CrossRef]
56. Gar, M.; Taw, A.; Ookawara, S. Enhancement of Photocatalytic Activity Journal of Environmental Chemical Engineering Enhancement of Photocatalytic Activity of TiO₂ by Immobilization on Activated Carbon for Degradation of Pharmaceuticals. *J. Environ. Chem. Eng.* **2016**, *4*, 1929–1937. [CrossRef]
57. Burak Ozkal Can, M.S. A Comparative Heterogeneous Photocatalytic Removal Study on Amoxicillin and Clarithromycin Antibiotics in Aqueous Solutions *Can. J. Water Technol. Treat. Methods* **2018**, *1*, 4–8.
58. Kawabata, K.; Sugihara, K.; Sanoh, S.; Kitamura, S.; Ohta, S. Photodegradation of Pharmaceuticals in the Aquatic Environment by Sunlight and UV-A, -B and -C Irradiation. *J. Toxicol. Sci.* **2013**, *38*, 215–223. [CrossRef]
59. Chang, M.T.; Wu, N.; Faqing, Z. A Kinetic Model for Photocatalytic Degradation of Organic Contaminants in a thin-film TiO₂ catalyst. *Water Res.* **2000**, *34*, 407–416. [CrossRef]
60. Cortés, J.A.; Alarcón-Herrera, M.T.; Villicaña-Méndez, M.; González-Hernández, J.; Pérez-Robles, J.F. Impact of the Kind of Ultraviolet Light on the Photocatalytic Degradation Kinetics of the TiO₂/UV Process. *Environ. Prog. Sustain. Energy* **2011**, *30*, 318–325. [CrossRef]
61. Choi, J.; Lee, H.; Choi, Y.; Kim, S.; Lee, S.; Choi, W.; Lee, J. Heterogeneous Photocatalytic Treatment of Pharmaceutical Micropollutants: Effects of Wastewater Effluent Matrix and Catalyst Modifications. *Appl. Catal. B* **2014**, *147*, 8–16. [CrossRef]
62. Finčur, N.L.; Krstić, J.B.; Šibul, F.S.; Šojić, D.V.; Despotović, V.N.; Banić, N.D.; Agbaba, J.R.; Abramović, B. Removal of Alprazolam from Aqueous Solutions by Heterogeneous Photocatalysis: Influencing Factors, Intermediates, and Products. *Chem. Eng. J.* **2017**, *307*, 1105–1115. [CrossRef]
63. AFNOR. Evaluation En Milieu Aqueux de La Biodégradabilité Aérobie ‘Ultime’ Des Produits Organiques Solubles. Méthode Par Analyse de Dioxyde Dégagé. 1994, T 90-306. Available online: <https://www.iso.org/fr/standard/42155.html> (accessed on 6 May 2022).
64. Melgoza, R.M.; Chew, M.; Buitrón, G. Start-up of a Sequential Anaerobic/Aerobic Batch Reactor for the Mineralization of p-Nitrophenol. *Water Sci. Technol.* **2000**, *42*, 289–292. [CrossRef]
65. American Public Health Association; American Water Works Association; Water Environment Federation (Eds.) *Standard Methods for Examination of Water and Wastewater*, 21st ed.; APHA-AWWA-WEF Publisher: Washington, DC, USA, 2005.
66. Kuhn, H.; Fösterling, H. Kinetics of Chemical Reactions. In *Principles of Physical Chemistry*; Wiley: West Sussex, UK, 2000.
67. GáborLente Facts and Alternative Facts in Chemical Kinetics: Remarks about the Kinetic Use of Activities, Termolecular Processes, and Linearization Techniques. *Curr. Opin. Chem. Eng.* **2018**, *21*, 76–83. [CrossRef]